Time-resolved exciton transfer in GaAs/$Al_xGa_{1-x}As$ double-quantum-well structures

R. Ferreira, P. Rolland, Ph. Roussignol,* and C. Delalande
Laboratoire de Physique de la Matière Condensée de l'Ecole Normale Supérieure, 24 rue Lhomond, 75230 Paris, France

A. Vinattieri, L. Carraresi, and M. Colocci
Dipartimento di Fisica and Laboratorio Europeo di Spettroscopie Non-Lineari, Università di Firenze, Largo Enrico Fermi, 2, 50125 Firenze, Italy

N. Roy, B. Sermage, and J. F. Palmier
Laboratoire de Bagneux, Centre National d'Etudes en Télécommunications, 196 avenue Henri Ravera, 92220 Bagneux, France

B. Etienne
Laboratoire de Microélectronique et de Microstructures, Centre National de la Recherche Scientifique, 196 avenue Henri Ravera, 92220 Bagneux, France
(Received 13 November 1991)

Transfer of excitons through a barrier is studied by means of time-resolved photoluminescence in a biased GaAs/$Al_xGa_{1-x}As$ asymmetric double-quantum-well structure. By tuning the external electric field, the dynamics of the system is investigated in the vicinity of the resonance between the first conduction subbands of the two wells. The excitonic nature of the tunneling process at low temperature is demonstrated. A nonlinear behavior of the interwell transfer is also observed when the appearance of a crossed exciton induces a dipolar electric field. The experimental curves are quantitatively compared with a theoretical simulation of the exciton-assisted tunneling process.

INTRODUCTION

Coupled-quantum-well (QW) structures represent one of the most widely used heterostructures to perform optical studies of carrier or exciton tunneling through a barrier in semiconductors. In the strong-coupling limit (small barrier width between the two QW's), the electronic levels becomes delocalized over the two wells.[1-3] A coherent excitation of the two levels arising from the coupling between the two wells can lead to the optical observation of oscillations of the photocreated wave packet.[4] In the weak-coupling regime (wide barrier width), carriers and excitons can be created in a given QW by a selective excitation of its levels and tunneling can occur to the adjacent QW if the tunneling time is shorter than the recombination time. The use of a simple system such as an asymmetric double-QW structure offers many advantages: The origin of the levels of the whole structure is easily tracked and the application of an electric field gives the opportunity of varying the resonance conditions between the levels of the adjacent wells.

By steady-state or time-resolved experiments, evidence of electron and hole tunneling has been given[5-14] and the calculated assisted-tunneling rates[15,16] are in good agreement with experimental data. Nevertheless, in the wide barrier regime, the excitonic nature of the transfer is often forgotten: in fact, although evidence for it has been reported by steady state experiments,[16,17] no agreement has yet been reached on whether, especially in time-resolved experiments, excitons transfer as a whole or rather free-electron and hole tunneling is observed.[17-19] Moreover, if the fundamental conduction and valence states are not localized in the same well, a so-called crossed exciton or indirect exciton can appear.[20-23] Considering the reduced overlap of the electron and hole wave functions, a long lifetime is expected for the crossed exciton.[24,25] Another consequence of this spatial separation of charges is the large induced electric dipole which may modify locally the applied electric field and therefore the dynamics of the transfer itself, as shown by Sauer, Thonke, and Tsang in steady-state experiments performed at very high excitation regime.[18]

In this paper, we present an experimental study of the effects of band alignment on the tunneling times of excitons in a biased asymmetric double-quantum-well structure. The tunneling times are measured, as a function of the applied electric field, around the resonance between the two fundamental electronic levels of the two wells. The excitonic nature of the transfer at low temperature is demonstrated. Two resonances are observed in the tunneling times when varying the electric field: they occur on both sides of the resonance, which would be predicted on the basis of the alignment of the electronic levels. Even for excitons, fast tunneling times (a few tens of ps) are measured at low temperature under resonant conditions. Finally, the transfer from a direct to a crossed exciton is strongly dependent on the excitation-intensity. Intensity-dependent recombination curves are measured and the observed nonlinear behavior is explained in terms of the appearance of a dipole due to the formation of the crossed exciton. The experimental curves are quantitatively compared with a theoretical simulation of the

exciton-assisted tunneling process.

The paper is organized as follows. The sample, experimental setups, and results are described in Sec. I. A theoretical simulation is developed and discussed in Sec. II. Section III is devoted to the interpretation of the results, and finally conclusions are drawn in Sec. IV.

I. EXPERIMENTAL RESULTS

A. Sample description and experiment

The sample used in our measurements consists in two GaAs quantum wells of different widths, 78 and 35 Å, respectively, separated by a 55-Å-thick $Al_{0.3}Ga_{0.7}As$ barrier. This double-quantum-well structure is embedded in the intrinsic 1-μm-thick $Al_{0.3}Ga_{0.7}As$ part of a p^+-i-n^+ junction (p^+-type substrate and 4000-Å n^+-type GaAs upper layer). Near the double-quantum-well structure, the $Al_{0.3}Ga_{0.7}As$ barrier is replaced by a (8 monolayers)/(4 monolayers) GaAs/AlAs superlattice, on a thickness of 600 Å, in order to improve the quality of the interfaces. Square mesas with a surface of 80×80 μm^2 are obtained by optical lithography and wet etching. Au-Ge-Ni/Au contacts are deposited on both the p^+-type back side and the n^+-type mesa top.

A picture of the relevant energy levels of the structure is shown in Fig. 1, where the levels of the wide well and the narrow well are indicated without or with a prime, respectively. By applying a voltage from -1 to -4 V, corresponding to an electric field in the range -37.5 to -70 kV cm^{-1}, it is possible to bring the fundamental electronic level $E1$ of the wide well and the fundamental $E'1$ level of the narrow well close to resonance (Fig. 1). At zero field, $E1$ is the fundamental conduction level of the system, while $E'1$ becomes the fundamental one after the resonance. The fundamental valence-band level remains $H1$, the first heavy-hole state of the wide well.

The measurements have been performed at $T=4$ or 2 K, keeping the sample fully immersed in liquid helium. cw measurements have been performed by standard dye laser and lock-in techniques. For the time-resolved measurements the optical excitation was provided by a pyridine dye laser synchronously pumped by the second harmonic of a Nd:YAG mode-locked laser with a 76-MHz repetition rate and 5-ps pulse duration. Part of the measurements was done with a dye laser synchronously pumped by an Ar^+-ion mode-locked laser; in this case the pulse duration was 3 ps and the repetition rate 82.3 MHz. The laser was focused on a 100-μm-diam spot and the photoluminescence (PL) signal was detected, in a backward geometry, by a Hamamatsu synchroscan streak camera after a 30-cm Jobin-Yvon monochromater or a 22-cm Spex double monochromator (1-meV resolution). The time resolution of the whole system was of the order of 15 ps. The PL decay curve for the crossed exciton has been measured using a time-correlated single-phonon-counting apparatus, providing a time resolution of 100 ps after numerical deconvolution for the instrumental response function. Time- and frequency-resolved spectra were recorded gating the signal from the time-correlated single-phonon-counting system at different delays with respect to the excitation pulses.

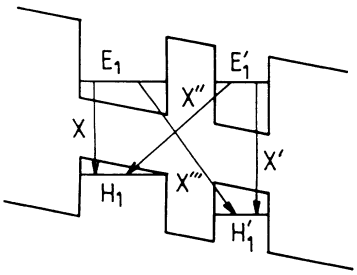

FIG. 1. Band diagram of the double-quantum-well structure with the schematic allowed excitonic transitions: X, X', X'', and X'''.

B. cw measurements

By tuning the laser energy below the first electron–heavy-hole transition of the thin QW, the wide well is selectively excited. The cw PL spectrum of the wide QW, obtained at low excitation density, is reported in Fig. 2 for different bias voltages. As clearly shown, the low-energy side of the PL line becomes more important when increasing the negative voltage and eventually two peaks appear for $V\leq-3.5$ V. At low voltage ($V\approx-1$ V), only the direct exciton (called X) is observed. This exciton is related to the first electronic state E_1 and the first heavy-hole state H_1 of the wide QW (Fig. 1). At sufficient negative voltage ($V\approx-3.5$ V) a crossed exciton (labeled X'' in Fig. 1) appears. X'' is formed with a hole in the fundamental heavy-hole H_1 state of the wide QW and an electron in the fundamental conduction state E'_1 of the thin QW.[8] This makes possible the study of the transfer through the barrier from the direct exciton to the crossed one.

Note that the X''' crossed exciton related to the E_1 and

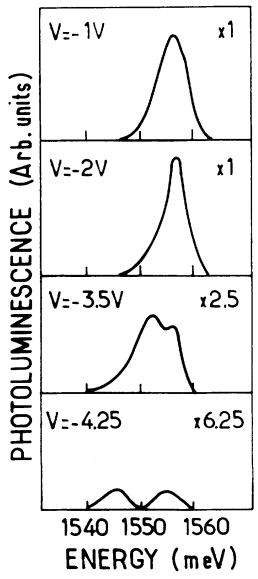

FIG. 2. cw photoluminescence spectra of the wide well at different applied voltages.

H_1' states is not observed experimentally, the fundamental hole level of the double quantum well remaining H_1 for all the range of applied voltages.

C. Exciton tunneling times at low excitation density

On one hand, when exciting above the narrow QW band gap, it is possible to study the decay time of the direct exciton (called X' in Fig. 1) when both carriers are localized in the thin QW. The exciton wavelength is then matched to the E_1'-L_1' optical transition.

On the other hand, when the excitation wavelength is chosen in order to match the transition between E_1 and L_1, the wide QW is selectively excited and the transfer of the X exciton towards the X'' can be studied.

In Fig . 3 the variation of the PL decay time, as a function of the applied voltage, is displayed for the X' exciton (squares) and the X exciton (circles). These data correspond to a set of experiments performed at low excitation power ($\approx 10^9$ carriers/cm^2 per pulse). As clearly shown in this figure, the dependence of the PL decay time on the applied voltage is quite different for the two excitons. The variation with voltage of the decay time of the X' exciton exhibits a minimum at $V=-2$ V ($\approx$40 ps). As far as the X exciton (circles) is concerned, for applied voltages between -1 and -2.5 V, the PL decay time from the wide QW shows results that are fairly constant ($\approx$220 ps); for higher voltages it increases and a maximum at $V=-3.2$ V ($\approx$350 ps) is observed followed by a minimum at $V=-4.1$ V ($\approx$20 ps). For sufficiently negative voltages, the PL decay time of the X'' exciton is also measured (Fig. 4). It is found around 10 ns and no significant dependence on the applied voltage (-4.5 V $< V < -3.5$ V) is observed.

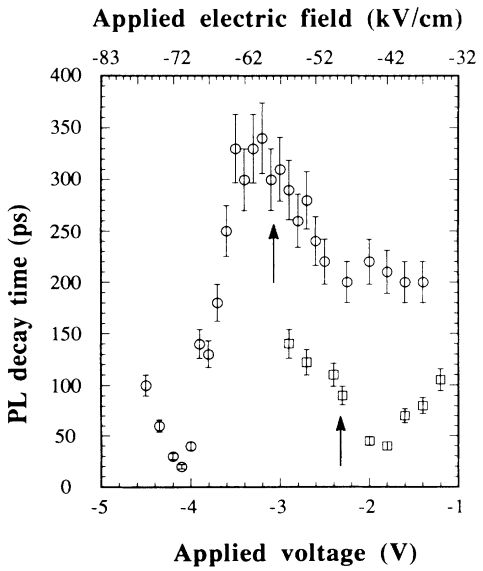

FIG. 3. Decay time of the photoluminescence of the wide well (circles) and of the narrow well (squares) as a function of the applied voltage at low excitation density. The arrows indicate the positions of the calculated R_1 and R_2 resonances (see Sec. III).

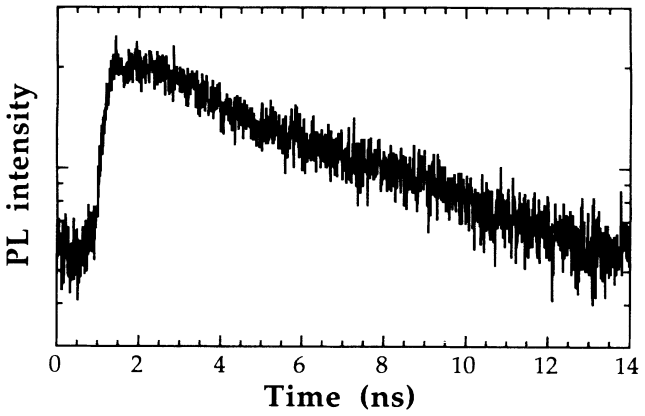

FIG. 4. Photoluminescence decay time of the crossed exciton X'' for an applied voltage of $V=-3.9$ V.

D. Excitation density dependence of the exciton transfer

Whatever the voltage is, the PL decay time of the X' line does not depend on the excitation power. The same independence is observed for the X line at low negative voltage. In this case, when the wide QW is selectively excited, the experimentally observed PL decay of the direct X exciton is closely related to the recombination of the isolated wide QW. On the contrary, at higher applied electric fields ($V<-3.2$ V) when the transfer process from direct to crossed exciton is possible, the PL decay curves of the wide QW appear strongly dependent on the excitation intensity, as shown in Fig. 5, for $V=-3.8$ V. In our experimental configuration, an excitation power of 1 mW corresponds roughly to a density of photocreated carriers of 10^{10}/cm^2. At low excitation intensity (0.3 mW), a fast decay of the PL is observed over more than one order of magnitude, followed by a weak slower one [Fig. 5(a)]. The data of Fig. 3 correspond to the decay time of the fast component. At moderate excitation intensity [1.3 mW: Fig. 5(b)], the PL decay still shows two components, but the relative magnitude of the fast component with respect to the slow one decreases; the fast component at short times is essentially the same as in Fig. 5(a). At higher excitation [6 mW: Fig. 5(c)], only a slow component is observable, and a further increase of the excitation intensity [11 mW: Fig. 5(d)] gives rise to a wide plateau, followed by a slow decay in the same range as in Fig. 5(c).

II. THEORETICAL FRAME

A. Electron and hole states

In the following, we will be concerned with the first few optical transitions near the fundamental gap. Only a few conduction- and valence-band levels are present in the structure at zero bias (well widths <100 Å). Figure 6 shows the theoretical variation as a function of the external electric field of the four principal band-to-band edges and the four corresponding 1S-like "ground" exciton

states for the (78 Å)/(55 Å)/(35 Å) structure described in Sec. I. The details of the calculations have been presented elsewhere,[16] and in the following we will discuss the same results in terms of a simpler model.

For simplicity, we assume a tight-binding description of the biased asymmetric double quantum well (ADQW).[15,26] The structure is initially considered as two noninteracting wells, and we retain only the ground electronic (ε_1 and ε_1') and hole (h_1 and h_1') levels of each isolated well. Unprimed and primed quantities refer to the wide and narrow wells, respectively.

Both the external electrostatic potential and interwell (tunnel) coupling due to the finite barrier width must be considered when searching for the actual ADQW levels (E_1, E_1', H_1, and H_1'). In a first approximation the electric field F only shifts in a rigid way the isolated well energies ε_1 and ε_1' (if we focus on the conduction-band states). Taking the origin of the electrostatic potential at the center of the barrier, we then have

$$\varepsilon_1(F)=\varepsilon_1(F=0)+eFz_w \ , \tag{1a}$$

$$\varepsilon_1'(F)=\varepsilon_1'(F=0)+eFz_N \ , \tag{1b}$$

where $z_w=-(L+b)/2$, $z_N=(L'+b)/2$, with L, L', and b corresponding to the wide well, narrow well, and barrier widths, respectively. The two wells are disposed as shown in Fig. 1, so that, for positive F, $\varepsilon_1(F)$ [$\varepsilon_1'(F)$] decreases (increases) with increasing electric field. The corresponding wave functions are given by

$$\varphi_{\varepsilon_1}(z)=\varphi_{\mathrm{loc},L}(z-z_w) \ , \tag{2a}$$

$$\varphi_{\varepsilon_1'}(z)=\varphi_{\mathrm{loc},L'}(z-z_N) \ , \tag{2b}$$

where $\varphi_{\mathrm{loc}}(z)$, the ground-state solution of the unbiased isolated quantum-well problem, is strongly localized in the quantum-well region. We neglect in this simple description the corrections on the energies and wave functions due to the intrawell quantum confined Stark effect,[18] which are small for thin wells.

Eigenstates of the *whole* structure result from the tunnel coupling of the two *localized* (in different wells) states. An estimation of the strength of this coupling is given by the parameter $\lambda_C=|\lambda_1\lambda_2|^{1/2}$, where $|\lambda_1|$ and $|\lambda_2|$ are the transfer integrals:

$$|\lambda_1|=V_C\langle\varphi_{\mathrm{loc},L}(z-z_W)|\varphi_{\mathrm{loc},L'}(z-z_N)\rangle_{\text{wide well}} \ , \tag{3a}$$

$$|\lambda_2|=V_C\langle\varphi_{\mathrm{loc},L}(z-z_W)|\varphi_{\mathrm{loc},L'}(z-z_N)\rangle_{\text{narrow well}} \ . \tag{3b}$$

The integration has to be performed over the well regions, and V_C is the conduction-band confining potential. $|\lambda_1|$ and $|\lambda_2|$ vary exponentially with the barrier width

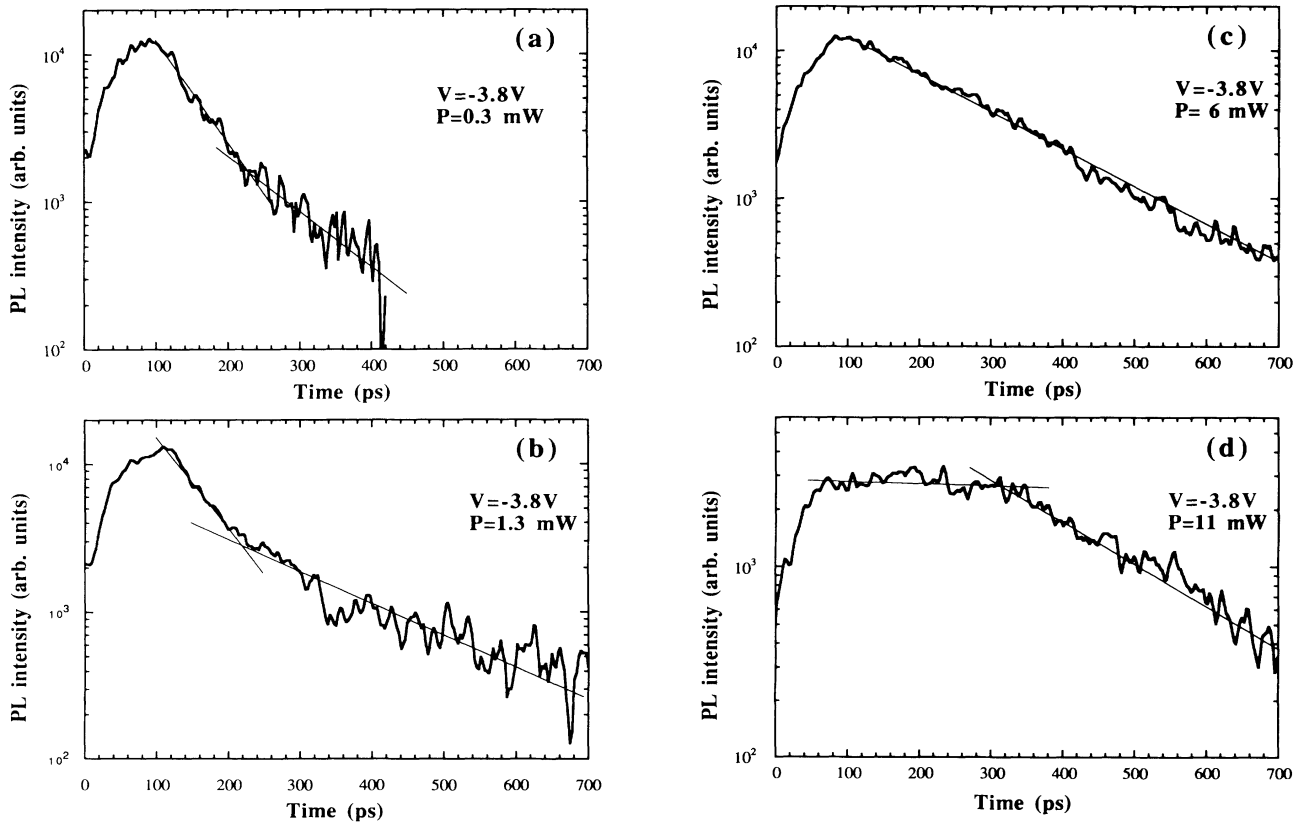

FIG. 5. Measured photoluminescence decay of the wide well at $V=-3.8$ V for increasing excitation powers: 0.3 mW (a), 1.3 mW (b), 6 mW (c), and 11 mW (d). 1 mW corresponds to an estimated density of 10^{10} cm^{-2} photocreated carriers.

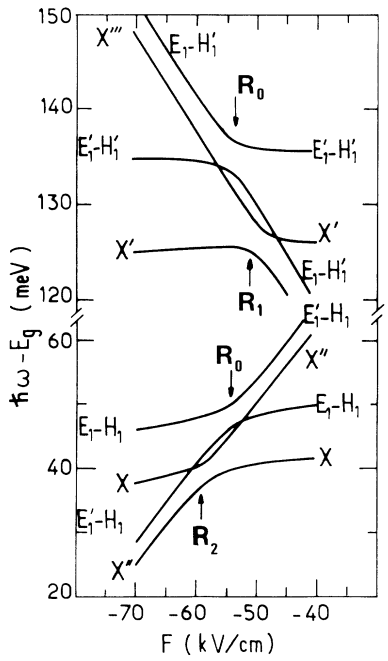

FIG. 6. Calculated electric-field dependence of the band-to-band transitions (e.g., E_1-H_1) and $1S$ excitonic transitions (e.g., X). Arrows show the resonances expected for the tunneling process: R_1 for the X'-X''' couple, R_2 for the X-X'' couple and R_0 for the band-to-band resonance.

and $\lambda_C \to 0$ when $b \to \infty$. The tight-binding energy matrix reads

$$\begin{bmatrix} \varepsilon_1 - E & -|\lambda_1| \\ -|\lambda_2| & \varepsilon_1' - E \end{bmatrix} \begin{bmatrix} A \\ A' \end{bmatrix} = \begin{bmatrix} 0 \\ 0 \end{bmatrix} . \tag{4}$$

The corresponding wave functions for $E = E_1$ and $E = E_1'$, the two ADQW eigenenergies, are

$$\varphi_E(z) = A\varphi_{\varepsilon_1}(z) + A'\varphi_{\varepsilon_1'}(z) , \tag{5}$$

where the coefficients A and A' ($A^2 + A'^2 \approx 1$) account for the mixing of the two decoupled ε_1 and ε_1' states.

For a given barrier width, another important parameter is the energy "detuning" $\Delta\varepsilon(F) = |\varepsilon_1(F) - \varepsilon_1'(F)|$. Whenever $\Delta\varepsilon(F) \gg 2\lambda_C$, the ADQW energies and wave functions are given essentially by the two decoupled solutions ($|A|, |A'| \approx 0$ or 1). On the other hand, whenever $\Delta\varepsilon(F) \leq 2\lambda_C$, the tunnel interaction effectively mixes the two localized states, and each one of the two ADQW eigenstates spreads over the whole ADQW structure [$|A| \approx |A'| \approx 1/\sqrt{2}$ if $\Delta\varepsilon(F) \approx 0$].

The last inequality [$\Delta\varepsilon(F) \leq 2\lambda_C$] can be rewritten $|\Delta F| = |F - F_0| \leq 2\lambda_C/ed = |\Delta F_c|$, where F_0 is the resonance field defined by $\varepsilon_1(F_0) = \varepsilon_1'(F_0)$, $F_0 < 0$, and d is the distance between the center of the two wells. For field values in that interval the ADQW energies E_1 and E_1' deviate from the isolated well values ε_1 and ε_1' and, in particular, the crossing $\varepsilon_1 = \varepsilon_1'$ at $F = F_0$ is replaced by an anticrossing with an energy splitting $|\Delta E(F_0)| = 2\lambda_C$. A variation of the external electric field by $|\Delta F_c|$ near the resonant value F_0 allows the change from a situation of two quasidecoupled wells to a situation of two strongly interacting wells (resonance R_0). Note that for thick barriers ($b > 100$ Å) or very thin barriers ($b \leq 20$ Å), $|\Delta F_c|$ is either extremely small or very large, and no experimental resonant features are expected in any physical property depending on the spatial extension of the ADQW states when varying the external field. In the thin-barrier case, the resonances would be very smooth; in the wide-barrier case, the broadening of the lines due to the inhomogeneity of the structure washes out the resonance. For the (78 Å)/(55 Å)/(35 Å) structure described above, we find $|\Delta E(F_0)| \approx 3$ meV, $|\Delta F_c| \approx 3$ kV/cm, and $F_0 \approx -54$ kV/cm.

For the valence states, similarly, we have

$$h_1(F) = -|h_1(F=0)| - eF|z_W| , \tag{6a}$$

$$h_1'(F) = -|h_1'(F=0)| + eFz_N , \tag{6b}$$

and the energy crossing $h_1 = h_1'$ is located in the positive field region. The corresponding hole wave functions are given by

$$\chi_{h_1}(z) = \chi_{\mathrm{loc},L}(z - z_W) , \tag{7a}$$

$$\chi_{h_1'}(z) = \chi_{\mathrm{loc},L'}(z - z_N) , \tag{7b}$$

where $\chi_{\mathrm{loc}}(z)$ is the ground-hole solution of the unbiased isolated quantum-well problem. For negative fields we have $h_1(F) > h_1'(F)$, and the hole wave functions $\chi_{h_1}(z)$ and $\chi_{h_1'}(z)$ are strongly localized in the wide and narrow wells, respectively. Since for hole states $\lambda_h \approx 0$, a good approximation is to consider the two decoupled solutions [Eq. (7)] as solutions of the ADQW problem.

Four band-to-band transitions are then obtained by combinating the two hole levels and the two electronic levels. Far from the resonance R_0 region ($|F - F_0| \gg |\Delta F_c|$) one has both direct and crossed edges; direct (crossed) transitions occur between a hole and an electron located in the same (different) well: E_1-$H_1 \approx \varepsilon_1$-$h_1$ and E_1'-$H_1' \approx \varepsilon_1'$-$h_1'$ (E_1'-$H_1 \approx \varepsilon_1'$-$h_1$ and E_1-$H_1' \approx \varepsilon_1$-$h_1'$). We would like to stress here two features.

(i) The fundamental transition associated to each hole level changes from a direct one to a crossed one (or vice versa) as we go from one side to the other of the resonance field F_0 (R_0 in Fig. 6). In particular, when $F_0 < F < 0$, the first energy edge corresponds to the intra-wide-well transition ε_1-h_1, whereas for $F < F_0$ it corresponds to the interwell ε_1'-h_1 one. As we will see below, the fact that for large negative electric fields the ground electronic transition corresponds to a crossed one is crucial for the understanding of the experimental results.

(ii) The second remark concerns the interband optical absorption in an ADQW under off-resonance condition. This absorption is essentially an intrawell process (vertical transition in the real space). Indeed, it strongly depends on the overlap of the electron and hole wave functions, which is almost negligible for carriers in different wells (interwell overlaps are roughly smaller by a factor

$\lambda_C/V_C \ll 1$ with respect to the intrawell ones). Since in addition the intrawell edges are energetically well separated, it turns out that for such electric-field values the spatial origin of the optical process can be tracked back, which is very convenient from a practical point of view.

On the other hand, in the anticrossing region "interwell" and "intrawell" contributions to the optical properties compete. In fact, due to the increasing spread of the eigenstates through the whole structure, "inter" and "intra" become meaningless as F approaches F_0. In addition, when the energy mismatch between the two ADQW levels is of the order of a few meV, the experimental optical resolution of the two contributions becomes difficult because of the broadening of the lines.

The oscillator strength f_r for interband transitions is proportional to the square of the electron and hole wave function overlap:

$$f_r \propto |[A\langle\varphi_{\varepsilon_1}(z)|\chi_{h_1}(z)\rangle + A'\langle\varphi_{\varepsilon_1'}(z)|\chi_{h_1}(z)\rangle]|^2 . \quad (8)$$

Before discussing exciton states, let us consider in detail the variation with the electric field of the oscillator strength f_r for an electron-hole pair. Let us take, for instance, the E_1-H_1 and E_1'-H_1 transitions. For $F_0 \ll F < 0$, the E_1-H_1 transition is the fundamental one and $f_r(E_1\text{-}H_1)$ is almost independent on F, whereas $f_r(E_1'\text{-}H_1)$ varies exponentially with the energy difference ΔE, and $f_r(E_1'\text{-}H_1) \ll f_r(E_1\text{-}H_1)$. As F approaches F_0 ($F_0 < F$), the electron wave function becomes delocalized and $f_r(E_1\text{-}H_1)$ decreases [$f_r(E_1'\text{-}H_1)$ sharply increases], reaching a minimum value (maximum value) for $F = F_0$, which is roughly a half of its off-resonance value [roughly equal to $f_r(E_1\text{-}H_1)$, respectively], since the wave function associated with E_1 delocalizes into the narrow well by at most a factor $1/\sqrt{2}$. For $F < F_0$, the opposite trend is observed. This behavior of f_r as a function of F is also observed for excitons (see below), and turns out to be important for the understanding of both cw and time-resolved PL experiments.

B. Exciton states

In the simplest approximation, an exciton state (let us focus on the 1S-like "ground" exciton state) can be assigned to each of the four band-to-band edges considered above. In the following, they will be labeled by X, X', X'', and X'''. The exciton energies read

$$\varepsilon_X(F) = \varepsilon_1(F) - h_1(F) - R_X , \quad (9a)$$

$$\varepsilon_{X'}(F) = \varepsilon_1'(F) - h_1'(F) - R_{X'} , \quad (9b)$$

$$\varepsilon_{X''}(F) = \varepsilon_1'(F) - h_1(F) - R_{X''} , \quad (9c)$$

$$\varepsilon_{X'''}(F) = \varepsilon_1(F) - h_1'(F) - R_{X'''} , \quad (9d)$$

where R_X, $R_{X'}$, $R_{X''}$, and $R_{X'''}$ are the respective electric-field-independent binding energies. The corresponding wave functions can be taken as[26]

$$\Psi_X = \varphi_{\varepsilon_1}(z_e)\chi_{h_1}(z_h)N_X \exp(-\rho/\lambda_X) , \quad (10a)$$

$$\Psi_{X'} = \varphi_{\varepsilon_1'}(z_e)\chi_{h_1'}(z_h)N_{X'} \exp(-\rho/\lambda_{X'}) , \quad (10b)$$

$$\Psi_{X''} = \varphi_{\varepsilon_1'}(z_e)\chi_{h_1}(z_h)N_{X''} \exp(-\rho/\lambda_{X''}) , \quad (10c)$$

$$\Psi_{X'''} = \varphi_{\varepsilon_1}(z_e)\chi_{h_1'}(z_h)N_{X'''} \exp(-\rho/\lambda_{X'''}) , \quad (10d)$$

where λ_i ($i = X, X', X'', X'''$) is a variational parameter that minimizes the exciton energy and $N_i = (2/\pi\lambda_i^2)^{1/2}$ a normalization constant.

Due to the very different energies between the levels h_1 and h_1' (at $F < 0$), the four excitons above can be divided in two groups: on one hand, X and X'', both associated with the ground hole state of the wide well (h_1); on the other, X' and X''', both associated with the ground hole state centered on the narrow well (h_1'). Each hole level originates a direct and a crossed exciton, corresponding to the pairing of such a hole either with an electron localized in the same well (direct) or in the other one (crossed). Due to the spatial separation of the carriers, the binding energies of the crossed states are considerably smaller than the direct ones [for instance, for the (78 Å)/(55 Å)/(35 Å) system, $R_X \approx 8.3$ meV and $R_{X''} \approx 3.5$ meV].

Let us consider the X and X'' states. According to Eqs. (9) they will cross at $F_2 = [\varepsilon_1(F=0) - \varepsilon_1'(F=0) - R_X + R_{X''}]/ed = F_0 - [R_X - R_{X''}]/ed$. In the same way the X' and X''' levels cross for $F_1 = F_0 + [R_{X'} - R_{X'''}]/ed$. Due to the different binding energies of the direct and crossed excitons, the two excitonic resonances (hereafter called R_1 for the X'-X''' couple and R_2 for the X-X'' couple) will correspond to electric field values F_1 and F_2 shifted with respect to F_0; this shift turns out to be negative for the X-X'' couple and positive for the X'-X''' couple: $F_2 < F_0 < F_1 < 0$. The observation of two sharp features in the variation of the relative intensities of the cw PL lines of an ADQW system as a function of F (and around F_0) has been recently claimed as strong evidence of the excitonic nature of these resonances.[16]

In order to evaluate the tight-binding exciton energies E_X, $E_{X'}$, $E_{X''}$, and $E_{X'''}$ we consider the two couples (X,X'') and (X',X''') separately. The tight-binding exciton matrix has the same form as in Eq. (4) for pure electronic states. ε_1 and ε_1' must be replaced by ε_1-h_1-R_X and ε_1'-h_1-$R_{X''}$ for the X and X'' excitons, respectively, and in a similar way for the X',X''' couple. In doing so, we neglect off-diagonal terms accounting for the coupling of the X-X'' excitons (or X'-X''' excitons) due to the Coulombic interaction, found to be much smaller than λ_C. The corresponding exciton wave functions are

$$\Psi_{X,X''} = \alpha\Psi_X + \beta\Psi_{X''} \quad (\alpha^2 + \beta^2 \approx 1) , \quad (11a)$$

$$\Psi_{X',X'''} = \gamma\Psi_{X'} + \delta\Psi_{X'''} \quad (\gamma^2 + \delta^2 \approx 1) , \quad (11b)$$

where the four coefficients [like A and A' in Eq. (5)] account for the mixing of the different excitons and deviate significantly from the 0 or ± 1 only for field values near F_1 and F_2. Then, the field induced anticrossing of the exciton states (for a fixed hole state) is associated with the corresponding electronic state (between E_1 and E_1' at F_0); moreover, in the tight-binding approximation, the energy splittings at the respective resonances are roughly the

same for both excitons and electrons:

$$|E_X(F_2)-E_{X''}(F_2)|\approx|E_1(F_0)-E_1'(F_0)|$$
$$\approx|E_{X'}(F_1)-E_{X'''}(F_1)| . \quad (12)$$

Most of what has been said before concerning the four band-to-band transitions is also valid for excitons, and, in some sense, concerns primarily excitons. Indeed, both optical absorption and PL lines of the ADQW at low temperatures are dominated by excitonic features. Since an exciton can be simply visualized as an *interacting* electron-hole pair, all of what has been said in items (i) and (ii) of Sec. II A is also valid for excitons.

As has been pointed out, the exciton recombination time displays a variation with the electric field around the fields F_2 (X-X'') or F_1 (X'-X'''). For the X-X'' states we have

$$\tau_{r(X,X'')}\approx\left|\int dz_e \Psi_{X,X''}(z_e, z_h=z_e, \rho=0)\right|^{-2}$$
$$=|[N_X\alpha\langle\varphi_{\varepsilon_1}(z)|\chi_{h_1}(z)\rangle$$
$$+N_{X''}\beta\langle\varphi_{\varepsilon_1'}(z)|\chi_{h_1}(z)\rangle]|^{-2} . \quad (13)$$

We show in Fig. 7 (solid line) the variation with the external applied voltage of the calculated recombination time of the direct exciton X. We have taken an intrawide-well recombination time of 220 ps measured at $V\approx-2$ V. For fields $F_2<F$ (or -3.2 V$<V$), X corresponds to the fundamental exciton level of the couple X-X''. It corresponds to the upper exciton level for fields $F<F_2$ (or $V<-3.2$ V). As discussed at the end of Sec. II A the oscillator strength f_r decreases near $F=F_0$ due to the spatial delocalization of the *electronic* wave functions. In the same way, the increase of the radiative recombination time near $F=F_2$ is due essentially to the spatial delocalization of the *exciton* wave function in the anticrossing region.

In the off-resonant case, the crossed recombination probability $1/\tau_{r(X,X'')}$ is much smaller than the direct one. Intrawell recombination times are of the order of a few hundreds of ps, while for crossed processes $\tau_{r(X,X'')}$ is in general of the order or longer than 10^4 ps. That explains why a crossed PL signal has been only observed when the ground interband transition is a crossed one. In fact, a high population of electron-hole pairs (excitons) is needed to compensate for the small recombination rate per couple. As we will see below, interwell assisted scatterings are eventually able to convert a crossed (direct) pair into the direct (crossed) one associated with the same hole level before a crossed (direct) recombination can occur. Let the crossed exciton correspond to the fundamental one; if interwell scatterings are able to bring a photocreated direct pair into a crossed one before an intrawell decay (this happens for scattering times shorter than the direct recombination time), then, at low temperature, a crossed PL line is expected.

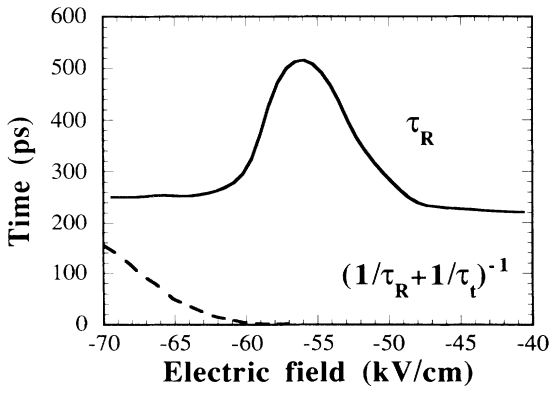

FIG. 7. Solid line, calculated radiative recombination time of the X exciton as a function of the applied voltage. Dotted line, field dependence of the calculated PL decay time of the wide well, taking into account radiative recombination and tunneling processes.

Note, finally, that the final binding energies of the four excitons are field dependent in the tight-binding approximation. In fact, if we define

$$R_X(F)=E_1(F)-H_1(F)-E_X(F) , \quad (14)$$

$R_X(F)$ approaches (deviates from) the decoupled value R_X for field values $|F-F_2|\gg|\Delta F_c|$ ($|F-F_2|\leq|\Delta F_c|$). In particular, $R_X(F)$ [$R_{X''}(F)$] should reach a minimum (maximum) value around $F=F_2$. The recombination time and the binding energy show opposite variations with F, as expected (the more the exciton is bound, the smaller the radiative decay time).

C. Assisted interwell transfer

Assisted relaxations in biased double quantum wells have been extensively discussed (see, for instance, Ref. 15, and references cited therein). Both elastic (ionized impurities, interface roughness) and inelastic (acoustical and optical phonons) processes have been shown to substantially broaden the excited eigenstates, and, in particular, couple states centered in different wells for the intermediate barrier thicknesses (b large enough to ensure a preferential localization of the wave functions in one of the two wells, but not as large to make the interwell overlap negligible; i.e., 30 Å$\leq b\leq$80 Å).

Figure 8 displays the impurity-assisted exciton transfer times for the (78 Å)/(55 Å)/(35 Å) structure (dashed-dotted curve, X-X'' couple; dashed curve, X'-X''' couple). For comparison, we show also the results for independent electrons (solid curve). As discussed in Sec. II B, when excitons are taken into account the position of the resonance in the tunneling process is shifted, with respect to the field corresponding to the band-to-band resonance R_0 to a higher negative value of the electric field for the X-X'' couple, and to a smaller negative value for the X'-X''' couple. The tunneling times calculated for independent electrons seem to be more or less one order of magnitude shorter than the exciton tunneling times. The results in Fig. 8 were obtained in the framework of the exciton states presented in Ref. 17. We consider elastic intersubband processes assisted by ionized impurities supposed to sit on the two inverted interfaces of the structure, with an areal concentration of 10^{11} cm^{-2}. The ini-

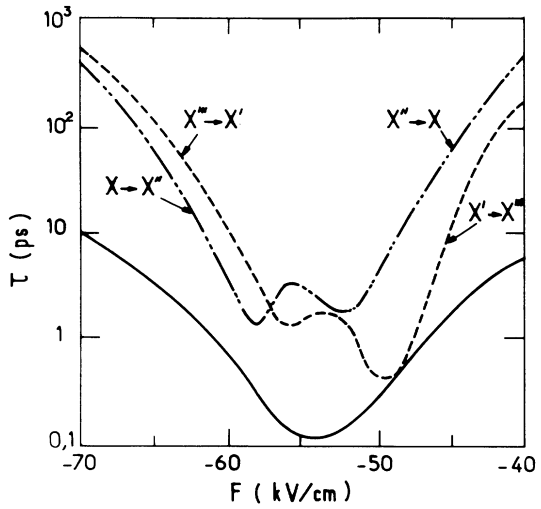

FIG. 8. Electric-field dependence of the impurity assisted tunneling times for the [(75 Å)/(55 Å)/(35 Å)] ADQW structure. Dotted line, transfer between the X' and X''' excitons. Dashed-dotted line, transfer between the X and X'' excitons. Solid line, tunneling time without excitonic effects.

tial state is always taken to be a $1S$-like state with vanishing in-plane wave vector ($\mathbf{K}_{\perp(\text{c.m.})}=0$) in the upper exciton branch and we compute, in the Born approximation, the time necessary for such an exciton to undergo impurity-induced transitions that conserve the total energy towards all possible states of the lower branch. For high (small) negative fields, the transfer converts a direct exciton into a crossed one for the X-X'' couple (the X'-X'' couple). Detailed calculations of the field-induced deformation of the exciton wave functions reveal that the X-X'' and X'-X''' resonances take place at the electric-field value where the transfer time has an absolute minimum.[17]

The results presented in Fig. 8 correspond to scattering times that couple exciton states formed by the same hole level ($X \leftrightarrow X''$ or $X' \leftrightarrow X'''$). For the X-X'' couple, the hole state H_1 is the fundamental one. Thus only the electron effectively transfers, whereas the hole only participates as a spectator. The differences between the dashed-dotted and solid curves are therefore due to the correlated motion of the electron-hole pair in the exciton state. Note, however, that for the X' direct exciton both the electron E_1' and hole H_1' levels involved are one-particle excited states. Thus, the electron and hole can transfer successively via assisted scatterings. So, for the X' states there is a symmetric process to the one presented in Fig. 8 (dashed curve) and for which only the hole effectively transfers. Such processes are much too complicated to be treated theoretically. We have shown[27] that the tunnel transfer of *independent holes* in biased ADQW systems are strongly dependent on the mixed nature of the valence states (heavy-hole–light-hole mixings). So we expect that such mixing effects should also be important when considering the tunnel transfer of *correlated holes*. However, as compared to the parabolic description we use, the theoretical consideration of exciton states in quantum well is enormously complicated when the real dispersion of the valence states is considered (see, for instance, Ref. 28 and references cited therein). Although quantitative results are not easily obtained, nevertheless, such considerations appear to be important for the interpretation of the experimental results concerning the X' excitons (see Sec. III). Finally, as stressed in Ref. 17, the one-step process $X' \rightarrow X$ has been found to be much less efficient than the ones involving an intermediate crossed exciton level.[17]

D. Rate equations

Simple rate equations are proposed in order to theoretically evaluate the variation with time of the intensity of the various PL lines. They incorporate pump rates for the direct X and X' excitons, direct and crossed (field-dependent) radiative recombination rates, and direct to crossed exciton transfers. Nonradiative processes are neglected. When X'' is the ground exciton state, the time-dependent rate equations for the areal density of the population of the X-X'' couple can be written as

$$dn_X/dt = -n_X/\tau_{r(X)} - (n_X - n_{X''}e^{-\beta\Delta E})/\tau_{t(X,X'')} + G_X(t) , \quad (15a)$$

$$dn_{X''}/dt = -n_{X''}/\tau_{r(X'')} + (n_X - n_{X''}e^{-\beta\Delta E})/\tau_{t(X,X'')} , \quad (15b)$$

where $\Delta E(F)=|E_X(F)-E_{X''}(F)|$; $\tau_{t(X,X'')}$ is the transfer time for the X-X'' couple, and $1/\beta = k_B T$ is the thermal energy, accounting for the thermally activated reverse transfer. $G_X(t)$ represents the pump rate, related to the excitation density D_S by

$$G_X(t) = (D_s/\tau_m)\exp(-t/\tau_m) , \quad (16)$$

where τ_m is the rise time of the direct luminescence. When X is the fundamental state, $(n_X - n_{X''}e^{-\beta\Delta E})$ has to be replaced by $(n_X e^{-\beta\Delta E} - n_{X''})$.

The three time constants are all electric-field dependent: in fact, $\tau_{t(X,X'')}(F)$ is given in Fig. 8 and both $\tau_{r(X)}(F)$ and $\tau_{r(X'')}(F)$ are calculated as discussed above. τ_m is taken equal to 50 ps, the measured value of the rise time of the photoluminescence from the wide well in the off-resonant region. The initial conditions are taken to be $n_X(t=0)=n_{X''}(t=0)=0$, for $F=F_{\text{ini}}$, the initial value of the electric field.

Let us consider $F_{\text{ini}} < F_2$. At $t=0$ a photogenerated density of carriers is injected in the wide well, which relaxes towards the direct subband edge with a characteristic time constant given by τ_m. Then, radiative recombination with a rate proportional to $1/\tau_{r(X)}(F_{\text{ini}})$ and transfer into the narrow well at a rate proportional to $1/\tau_{t(X,X'')}(F_{\text{ini}})$ can occur. Once the transfer begins, an induced dipole, due to the spatial separation of the electrons and the hole, appears, and an opposite field rises. This opposite field $F_{\text{opp}}(t)$ can be estimated to be

$$F_{\text{opp}}(t) = (e/\epsilon)n_{X''}(t) . \quad (17)$$

$F_{opp}(t)$ enters in the time evolution of n_X and $n_{X''}$ in a nonlinear way. It changes the local effective electric field in the ADQW region; this modifies the recombination and transfer times, as well as the energy difference ΔE, which all determine the evolution rate of n_X and $n_{X''}$ and consequently the evolution of F_{opp}. Since the induced opposite field is positive, the effective electric field $F(t)=F_{ini}+F_{opp}(t)$ approaches F_2.

In the following we will be interested in the different time dependences of the various PL lines for different pumping intensities. Let us take $F_{ini}=-67.5$ kV/cm (which corresponds to $V\approx -3.8$ V, as in Fig. 5). We also have $\Delta E_{ini}\approx 8$ meV, $\tau_{r(X)}\approx 250$ ps, $\tau_{r(X'')}\approx 10$ ns, and $\tau_{t(X,X'')}\approx$ 60 ps; $\tau_{t(X,X'')}$ is therefore smaller than $\tau_{r(X)}$ at $t=0$.

We will denote by $I(t)$ and $I''(t)$ the luminescence intensities of the X and X'' lines, defined by $I(t)=n_X/\tau_{r(X)}$ and $I''(t)=n_{X''}/\tau_{r(X'')}$, respectively. As pointed out before, when the energy difference ΔE is smaller than the spectral broadening of the PL lines (≈ 5 meV; see Fig. 2), the observed luminescence should be a sort of average of the two theoretical intensities I and I''. For a convenient comparison with experiment, we have also considered the time evolution of the total luminescence, defined as $I_{tot}(t)=I(t)+\alpha(t)I''(t)$, where $\alpha(t)$ accounts for the mixing of the PL lines [the time dependence of α is due to the time dependence of $F(t)$ and thus of ΔE].

We show in Fig. 9 the time evolutions of the PL intensities $I(t)$, $I''(t)$, and $I_{tot}(t)$ and of the induced opposite field $F_{opp}(t)$ in Fig. 10. Various excitation densities are considered: $D_s=1$, 5, 8.5, and 15×10^{10} cm^{-2}. The plotted PL intensities are all divided by D_s, and in the figures D_s appears in unity of 10^{10} cm^{-2}.

Before describing our theoretical results, let us first discuss two main pints concerning the solutions of Eqs. (15).

The opposite field. Due to the tunneling process, part of the photocreated direct excitons is converted into crossed ones. The opposite field initially increases with t. For a total field greater than F_2, the direct exciton level becomes the fundamental one and the $X\rightarrow X''$ transfer stops. In that case only $X''\rightarrow X$ processes are eventually possible and again force the structure to approach resonance R_2. So, $F_{opp}(t)$ is a bounded function of time: $0\le F_{opp}(t)\le |F_{ini}-F_2|=F_{max}$(=9.5 kV/cm in our case). When $t\rightarrow\infty$ we also have to recover the initial situation at $t=0$, before the optical excitation: two depopulated exciton states and an internal electric field $F(t=\infty)=F_{ini}$.

As shown in Fig. 10, $F(t)$ initially increases with t and reaches a maximum value $F_{max}(D_s)\le F_{max}$ at a time

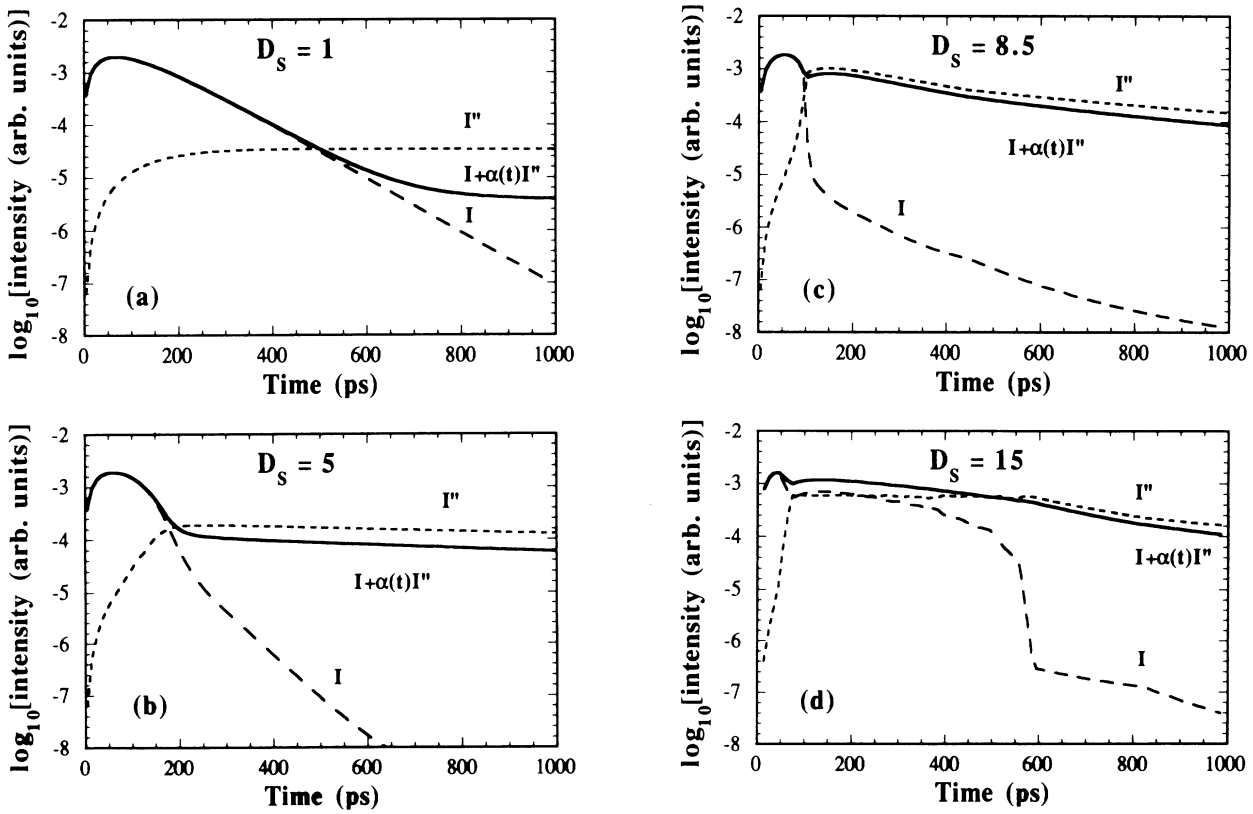

FIG. 9. Calculated PL decay of the direct (I) and crossed (I'') exciton for different excitation intensities: 10^{10} cm^{-2} (a), 5×10^{10} cm^{-2} (b), 8.5×10^{10} cm^{-2} (c), and 15×10^{10} cm^{-2} (d). The bold lines show $I_{tot}=I+\alpha(t)I''$. All the curves are normalized to the same initial intensity.

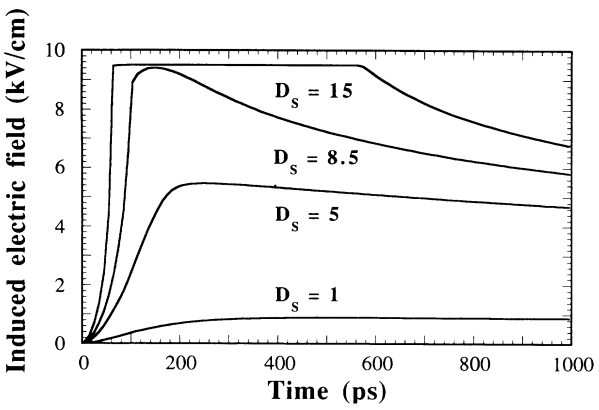

FIG. 10. Time evolution of the induced electric field by the excitonic transfer for four excitation densities: 10^{10}, 5×10^{10}, 8.5×10^{10}, and 15×10^{10} cm^{-2}.

$t_F(D_s)$, both depending on the excitation power. $F(t)$ eventually saturates at F_{max} for a short time interval and slowly decreases to zero when t goes to infinity.

The "thermal equilibrium" condition. Also important is the "thermal equilibrium" term $\Delta=(n_X-n_{X''}e^{-\beta\Delta E})$. Let us first suppose that the recombination times are every large ($\tau_r\to\infty$). The pumping rate $G_X(t)$ governs the evolution of the two populations for small times ($\Delta=0$ at $t=0$), whereas the evolution of n_X and $n_{X''}$ at longer times ($t\gg\tau_m$) is determined by Δ [since $G_X(t)\to0$]. Then, for $t\to\infty$ we get the stationary solutions

$$\Delta=n_X-n_{X''}e^{-\beta\Delta E}=0\ ,\qquad n_X+n_{X''}=D_s\ . \tag{18}$$

However, we know that the F_{opp} and $n_{X''}$ are not independent [Eq. (17)]. If, in addition, we remember that $0<F_{opp}(t)\le F_{max}$, then, from Eqs. (17) and (18) we deduce

$$D_s\le(1+e^{-\beta\Delta E})F_{max}/(e/\varepsilon)\approx7\times10^{10}\ \text{cm}^{-2}\ . \tag{19}$$

Thus, if D_s is not too high, the nonlinear condition relying on $n_{X''}$ and F_{opp} and the thermalization condition $\Delta=0$ are compatible.

At $t=0$, $\Delta(t)=0$; then, because of the pumping rate, $\Delta(t)$ increases at small times. Due to the interwell transfer it decreases rapidly and reaches a value very close to zero at a time $t_\Delta(D_s)$ that depend on the excitation density.

These considerations are still valid if the radiative recombinations are taken into account. This is due to the fact that the recombination times are always much greater than the transfer and τ_m times. The times $t_\Delta(D_s)$ are almost the same, and the "critical" density increases to 8.5×10^{10} cm^{-2} instead of $\approx7\times10^{10}$ cm^{-2} as in Eq. (19). We have also found numerically that for $D_s\le8.5\times10^{10}$ cm^{-2} (low and intermediate excitation regimes) $t_\Delta(D_s)\approx t_F(D_s)$; i.e., for a given D_s, the opposite field grows up whenever the condition $\Delta\approx0$ is not reached. For $t>t_\Delta(D_s)$ this quasiequilibrium condition remains and $F_{opp}(t)$ begins to decrease again.

For higher excitation powers ($D_s>8.5\times10^{10}$ cm^{-2}) we have chosen, for simplicity, to retain the coupled system given by Eqs. (15), subjected to the same (nonlinear) constraint imposed by the Eq. (17). For these densities $F_{opp}(t)$ rapidly saturates ($t_F\approx\tau_m$), and so $n_{X''}$ and ΔE, too. Only part of the injected excitons are needed to bring the structure to R_2, and pairs in excess accumulate in the ADQW.

We will now discuss separately the three density regimes: low, intermediate, and high excitation density.

Low excitation density. In Fig. 9(a) $D_s=10^{10}$ cm^{-2}. For low laser excitations the induced electric field is negligible compared to F_{max}: $F_{opp}<1.5$ kV/cm for $n_{X''}\le10^{10}$ cm^{-2} [see Eq. (17)]. The time evolution of the direct luminescence $I(t)$ is then determined by both τ_m and the parallel between $\tau_{r(X)}$ and $\tau_{t(X,X'')}$, evaluated at $F\approx F_{ini}$. At small times $I_{tot}(t)$ follows $I(t)$. When $I(t)$ becomes smaller than $I''(t)$, the total luminescence is due essentially to the crossed excitons, and displays a much slower decay. In Fig. 10 $F_{opp}(t)$ displays a very smooth maximum at $t_F\approx600$ ps.

Intermediate excitation density. In Figs. 9(b) and 9(c), $I(t)$ shows a fast rising time (≈50 ps) and a subsequent decay, which is steeper for $D_s=8.5\times10^{10}$ cm^{-2} than for $D_s=5\times10^{10}$ cm^{-2}. In the same way, $I''(t)$ rises more rapidly for increasing excitation powers. If the induced dipole field was not taken into account, an increase of D_s should proportionally increase both n_X and $n_{X''}$. However, as $n_{X''}$ increases, F varies and, since the transfer time decreases continuously as F approaches F_2, the transfer rate increase and so tends to increase $n_{X''}$ even more. Reversely, the direct luminescence decreases faster (at small decay times) with increasing excitation intensity. Thus, up to $t=t_F$ the time evolution of I and I'' is primarily determined by the induced dipole, which forces the structure to approach the resonance field F_2 as much as possible. In fact, the reverse transfer and the induced dipole are both proportional to $n_{X''}$ and tend to produce opposite effects, so that for longer delay times ($t>t_F$), when the quasiequilibrium is reached ($\Delta\approx0$), both $I(t)$ and $I''(t)$ show a slow decrease with time [Figs. 9(b) and 9(c)]. In this intermediate density regime $t_F\approx t_\Delta\ge\tau_m$, and a two-slope decrease of $I(t)$ is theoretically obtained. The time corresponding to the transition from the first slope to the other is in numerical agreement with the time t_F and t_Δ defined above. In Fig. 9(b) $t_F\approx200$ ps and in Fig. 9(c) $t_F\approx120$ ps (see Fig. 10). The higher the excitation density is, the smaller t_F. As far as the total luminescence is concerned, the higher D_s is, the more rapidly I_{tot} is dominated by $\alpha(t)I''(t)$.

High excitation density. In Fig. 9(d) $D_s=15\times10^{10}$ cm^{-2} and both $I(t)$ and $I''(t)$ or $I_{tot}(t)$ display an almost stationary behavior at small times (plateaus of nearly constant intensities). We attribute this behavior to the excess pairs present in the structure. For $t>600$ ps, $I''(t)$ shows a slow decay, whereas $I(t)$ rapidly decreases to very small values. We have checked numerically that

$\Delta(t)$ exhibit a slow decrease with time and $t_\Delta \approx 600$ ps $\gg t_F \approx \tau_m$. So, in the framework of our simple model, the break in $I(t \approx t_\Delta)$ is associated with the passage of a nonequilibrium situation, with X pairs present in excess in the structure and a saturated population of X'' pairs, to a situation of quasithermal equilibrium for these two populations. All these aspects are in good qualitative (and also in some cases in good quantitative) agreement with the experimental results, as discussed in the following section.

III. DISCUSSION

A. Exciton tunneling times

Let us first consider the X' exciton. The measured decay time of the photoluminescence from the thin QW results to be the parallel between the recombination time of the X' exciton, characteristic of the isolated well, and its tunneling time towards the wide well. As the applied voltage increases from -1 to -3 V, due to the quantum confined Stark effect, the decreasing overlap of the electron hole wave functions causes a small increase of the X' recombination time. Hence the minimum (≈ 40 ps) of the PL decay time observed for an applied voltage of -2 V can be unambiguously attributed to a higher tunneling rate of the X' exciton. This minimum is not far from the resonance R_1 (defined in Sec. II and calculated at -2.3 V) where the X' and X''' levels anticross (see Fig. 11). More precisely, this resonance rather corresponds to the calculated resonance between the $1S$ state of the X' exciton and the continuum of the X''' exciton, where a resonance in the exciton transfer does occur.[16]

As far as the X exciton is concerned, the observation of the resonance R_2 is also expected when the X and X'' energy levels anticross (Fig. 11). According to calculations, this resonance occurs at $V = -3.05$ V; experimentally, a broad maximum is observed in the PL decay time of the X exciton as a function of the applied voltage, around $V \approx -3$ V (Fig. 3). This feature can be easily accounted for by the calculated variations of the radiative and tunneling times of the X exciton, as plotted in Fig. 7.

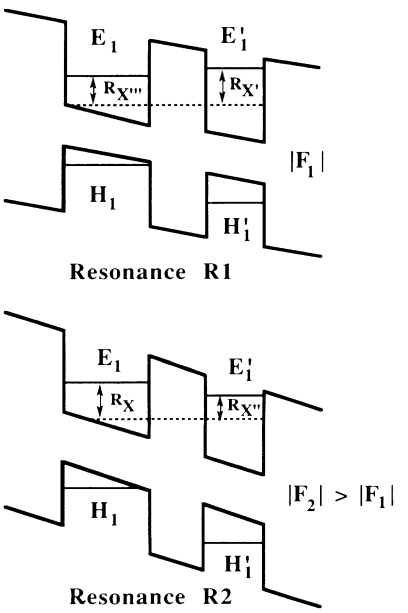

FIG. 11. Band diagram of the double-quantum-well structure at the X'-X''' resonance (resonance R_1) and at the X-X'' resonance (resonance R_2).

At low negative voltage, before the R_2 resonance (-2 V $< V < -1$ V), X is the fundamental level of the two wells, and its decay time is governed by the intrawell recombination channel of the isolated wide well. Increasing the negative voltage from $V = -2$ V, a low increase of $\tau_r(X)$ is experimentally observed, as predicted by the solid lines of Fig. 7. This is due to the small decrease of the overlap of the electron and hole wave functions.

When the resonance R_2 is reached ($V \approx -3$ V), the electronic part of the X and X'' excitons become delocalized over the two wells as detailed in Sec. II, and the eigenstates of the system are described by two $\Psi_{XX''}$-like wave functions. Close to R_2, we are experimentally unable to resolve spectrally the $\Psi_{XX''}$ states because of the broadening of the lines. So, even if the theory predicts an effective transfer between these two states, the PL decay time of the wide well remains equal to the recombination time of the $\Psi_{XX''}$ states. This time is calculated to be 530 ps (Fig. 7). A comparison with the measured value of 350 ps indicates that, even if the right order of magnitude is reached, nonradiative processes are still effective.

Increasing the negative voltage ($V < -3.2$ V, $F < 60$ kV/cm), the electronic parts of the X and X'' excitons become again more and more localized in the wide and the thin wells, respectively. Moreover, for $V < -3.2$ V, X'' becomes the fundamental state of the whole structure, so that an effective transfer is now expected from the X exciton toward the X'' one. Thus, when a sizable energy difference between the X and X'' lines appears, their spectral resolution, and then the measurement of their respective lifetimes, become possible. The minimum observed at $V = -4.1$ V corresponds effectively to a good experimental resolution between the X and X'' lines. The time measured here (20 ps) must now be compared to the corresponding point (160 ps) calculated as the dotted line of Fig. 7. In fact, our model considers only the resonance between the $1S$ level of the X exciton and the $1S$ level of the X'' exciton; resonances between the $1S$ level of the X exciton and the other levels of the X'' exciton ($2S, 2P, \ldots$, continuum) occur for applied voltages in the range -3 to -3.3 V. Obviously, these resonances will speed up the tunneling of the X exciton. For higher values of the applied voltage ($V = -4.1$ to -4.5 V), the increase of the X exciton tunneling time is related to the increased misalignment of the X and X'' levels.

In the intermediate region (-4 V $< V < -3.5$ V) the picture is much more complicated, due to the fact that the two excitonic lines cannot be observed independently. This region is not well described by our model of assisted tunneling. A proper description of the system should include an accurate treatment of the spectral broadening of the energy levels.

Our interpretation is well supported by the time- and

frequency-resolved spectra shown in Fig 12. The time evolution of the PL lines of the wide QW is shown on Fig. 12(a) for a -3.7-V bias voltage ($F=66.25$ kV/cm). At time $t=0$ only the X exciton recombination is observed. Then transfer occurs and the recombination of the X'' exciton appears (1-ns delay). Finally, for a 2-ns delay, only the recombination of the X'' exciton remains, in agreement with the measured decay time of the X'' exciton (Fig. 4). A significantly different result is obtained in Fig. 12(b) for a -3.2-V bias voltage ($F=60$ kV/cm) at the resonance R_2. Here, the PL line decays homogeneously, indicating that no transfer occurs.

One must note that a resonance can be observed either as a minimum or a maximum of the PL decay time. In general, a minimum is observed if the level populated by the interwell transfer process is rapidly depopulated by intrawell relaxation. This is the case when E_1'-E_2-like resonances are studied:[9,21] the populated level E_2 relaxes to the fundamental E_1 level. This is also valid in our case at the resonance R_1; the delocalized X'-X''' state relaxes towards the X state, which is the ground state of the whole heterostructure, through hole tunneling. As a matter of fact, the 40-ps tunneling time measured at $V=-2$ V is coherent with calculated values of hole nonresonant tunneling times through a 55-Å barrier with an energy mismatch of about 3 meV. In all of these cases a real transfer of population from one well to the other really occurs.

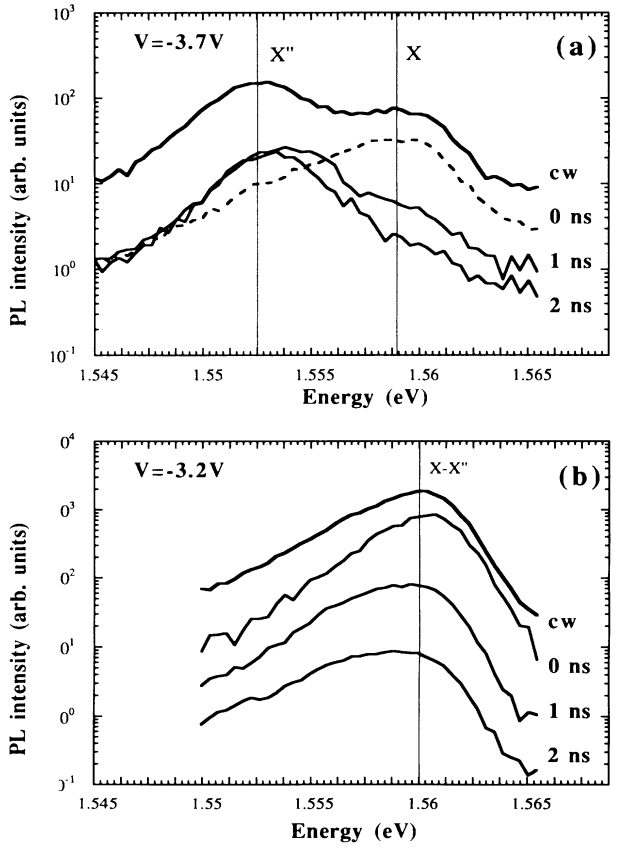

FIG. 12. Time- and frequency-resolved spectra of the wide-well photoluminescence for two applied voltages. (a) $V=-3.7$ V, "far" from the resonance R_2 where the X and X'' lines are spectrally resolved; (b) $V=-3.2$ V at the resonance R_2. cw spectra are also shown with bold lines.

On the other hand, at the R_2 resonance, the populated level is delocalized over the whole structure and has no way to relax rapidly. We then observe the recombination time of the delocalized $\Psi_{XX''}$ states.

We want to emphasize that here we have evidence that excitonic resonances are involved in the tunneling process at low temperature. Although the two processes are related to the E_1-E_1' lining up, the X'-X''' resonance (R_1) does not occur at the same voltage that the X-X'' resonance (R_2) does because of the difference between the excitonic binding energies: they are in the 10-meV range for the direct X and X' excitons, while they are in the 3-meV range for the crossed X'' and X''' excitons.

B. Excitation power dependence

Let us now turn to the nonlinear behavior observed in Fig. 5. It is qualitatively similar to the one predicted by the theory. However, note that the experimental results have to be compared with the calculated $I_{\rm tot}(t)=I(t)+\alpha(t)I''(t)$ of Fig. 9. For high excitation power, the induced electric field becomes large enough to bring the ADQW system close to the resonance R_2, where the X and X'' photoluminescence signals cannot be spectrally distinguished.

At $t=0$, for a voltage of $V=-3.8$ V, the internal electric field is -67.5 kV/cm. At low excitation power [Fig. 5(a)], the experimental PL decay is well reproduced by the curve displayed in Fig. 9(a). The measured decay (60 ps) of the fast component has to be compared with the calculated 90 ps. Note that even if the right order of magnitude is reached there is still a small discrepancy between the two results. It may arise from an oversimplification of our modeling of the assisted transfer process.

At moderate excitation powers [Fig. 5(b)], a two-slope time decay, with an increased magnitude of the slow component, is observed, as shown in Fig. 9(b). As the tunneling process occurs, a population of X'' excitons builds up and induces a dipolar electric field $F_{\rm opp}$ opposite from the applied one. This field brings the system close to resonance and speeds up the excitonic transfer; a value of about 40 ps is calculated for the PL decay time (50 ps measured). As the time proceeds, the X'' population decreases and goes away from resonance, and an apparent long decay time of the PL is observed.

At high excitation powers [Fig. 5(c)], the transfer is rapidly saturated, as explained in Sec. II; the reverse transfer becomes non-negligible and only a slow component is observable. Note that in the calculated PL decay curves of Fig. 9, an instantaneous response of the detection apparatus is assumed. A finite response time would smooth the initial part of the calculated curves and wash out the small discontinuities calculated at short decay times. Finally, in the very-high-excitation regime [Fig. 5(d)], the observation of a plateau, followed by a slow decay time, is in good agreement with the calculated $I_{\rm tot}(t)$ at very high D_s [Fig. 9(d)].

The agreement between the experimental observations and the calculated behavior is quite satisfactory. Nevertheless, slightly higher excitation intensities are used in the calculations. This may be due to the fact that our model considers only the effects of the induced electric dipole and does not take into account filling effects, which tend to slow down the tunneling process.[14]

IV. CONCLUSION

The excitonic nature of the interwell transfer at $T=4$ K has been unambiguously shown by means of time-resolved photoluminescence experiments in GaAs/$Al_{0.3}Ga_{0.7}As$ asymmetric double-quantum-well structures. Fast exciton tunneling times as short as a few tens of ps have been measured in near-resonant conditions for the electronic levels in the two quantum wells.

A nonlinear behavior of the PL temporal dynamics as a function of the excitation intensity has been observed and explained in terms of a simple model for the coupled exciton populations in the two wells, predicting a time dependence of the characteristic recombination constants due to the macroscopic electric dipole induced by the excitonic transfer. A good agreement between the experimental data and the calculated assisted transfer rates is obtained in the whole range 10^{10}–10^{11} cm^{-2} of the excitation density. Finally, a long decay time of the order of 10 ns for the PL originating from the crossed exciton has been experimentally measured, in good agreement with the expected reduction in the decay rate due to the decreased wave function overlap.

We want to remark that our experimental data and theoretical analysis clarify the exciton nature of tunneling. In QW heterostructures, at low temperature, interband optical absorption and radiative recombination are due to correlated electron-hole pairs. We show in this work that correlated electron-hole pairs also determine the interwell transfer of optical excitation in biased double-quantum-well structures at low temperature.

ACKNOWLEDGMENTS

We would like to thank M. Voos and G. Bastard for helpful discussions. The Laboratoire de Physique de la Matière Condensée is "Laboratoire associé à l'Université Paris VI et au CNRS." The Università di Firenze is affiliated to the Gruppo Nazionale di Struttura della Materia and to the Consorzio Interuniversitario di Fisica della Materia. One of us (R.F.) thanks the CAPES (Brasil) for financial support.

*Also at Dipartimento de Fisica and Laboratorio Europeo di Spettroscopie Non-Lineari, Università di Firenze, Largo Enrico Fermi, 2, 50125 Firenze, Italy.

[1]R. Dingle, A. C. Gossard, and W. Wiegman, Phys. Rev. Lett. **34**, 1327 (175).

[2]C. Delalande, U. O. Ziemelis, G. Bastard, M. Voos, A. C. Gossard, and W. Wiegman, Surf. Sci. **142**, 498 (1984).

[3]Y. J. Chen, E. S. Koteles, B. S. Elman, and C. A. Armiento, Phys. Rev. B **36**, 4562 (1987).

[4]K. Leo, J. Shah, E. O. Göbel, T. C. Damen, S. Schmitt-Rink, W. Schäfer, and K. Köhler, Phys. Rev. Lett. **66**, 201 (1991).

[5]D. Y. Oberli, J. Shah, T. C. Damen, C. W. Tu, T. Y. Chang, D. A. B. Miller, J. E. Henry, R. F. Kopf, N. Sauer, and A. E. Di Giovanni, Phys. Rev. B **40**, 3028 (1989).

[6]M. G. W. Alexander, W. W. Ruhle, R. Sauer, and W. T. Tsang, Appl. Phys. Lett. **55**, 885 (1989).

[7]B. Deveaud, F. Clerot, A. Chomette, A. Regreny, R. Ferreira, G. Bastard, and B. Sermage, Europhys. Lett. **11**, 367 (1990).

[8]M. Nido, M. G. W. Alexander, W. W. Ruhle, T. Schweizer, and K. Kohler, Appl. Phys. Lett. **56**, 355 (1990).

[9]M. G. W. Alexander, M. Nido,W. W. Ruhle, and K. Kohler, Phys. Rev. B **41**, 12 295 (1990).

[10]T. Matsusue, M. Tsuchiya, J. N. Schulman, and H. Sakaki, Phys. Rev. B **42**, 5719 (1990).

[11]B. Deveaud, A. Chomette, F. Clerot, P. Auvray, A. Regreny, R. Ferreira, and G. Bastard, Phys. Rev. B **42**, 7021 (1990).

[12]M. Nido, M. G. W. Alexander, W. W. Rühle, and K. Köhler, Phys. Rev. B **43**, 1839 (1991).

[13]Ph. Roussignol, M. Gurioli, L. Carraresi, M. Colocci, A. Vinattieri, C. Deparis, J. Massies, and G. Neu, Superlatt. Microstruct. **9**, 151 (1991).

[14]Ph. Roussignol, A. Vinattieri, L. Carraresi, M. Colocci, and A. Fasolino, Phys. Rev. B **44**, 8873 (1991).

[15]G. Bastard, C. Delalande, R. Ferreira, and H. W. Liu, J. Lumin. **44**, 247 (1989).

[16]F. Ferreira, H. W. Liu, C. Delalande, J. F. Palmier, and B. Etienne, Surf. Sci. **229**, 192 (1990).

[17]R. Ferreira, C. Delalande, H. W. Liu, G. Bastard, B. Etienne, and J. F. Palmier, Phys. Rev. B **42**, 9170 (1990).

[18]R. Sauer, K. Thonke, and W. T. Tsang, Phys. Rev. Lett. **61**, 609 (1988).

[19]T. B. Norris, N. Vodjdani, B. Vinter, C. Weisbuch, and G. A. Mourou, Phys. Rev. B **40**, 1392 (1989).

[20]S. Charbonneau, M. L. W. Thewalt, E. S. Koteles, and B. Elman, Phys. Rev. B **38**, 6287 (1988).

[21]T. B. Norris, N. Vodjdani, B. Vinter, E. Costard, and E. Böckenhoff, Phys. Rev. B **43**, 1867 (1991).

[22]C. Delalande and P. Rolland, Superlatt. Microstruct. **8**, 7 (1990).

[23]A. M. Fox, D. A. B. Miller, G. Livescu, J. E. Cunningham, and W. Y. Jan, Phys. Rev. B **44**, 6231 (1991).

[24]J. E. Golub, K. Kash, J. P. Harbison, and L. T. Florez, Phys. Rev. B **41**, 8564 (1990).

[25]A. Alexendrou, J. A. Kash, E. E. Mendez, M. Zachau, J. M. Hong, T. Fukuzawa, and Y. Hase, Phys. Rev. B **42**, 9225 (1990).

[26]G. Bastard, J. A. Brum, and R. Ferreira, in *Solid State Physics: Advances in Research and Applications,* edited by H. Ehrenreich and D. Turnbull (Academic, New York, 1991), Vol. 44, p. 229.

[27]R. Ferreira and G. Bastard, Europhys. Lett. **10**, 279 (1989).

[28]L. C. Andreani and A. Pasquarello, Phys. Rev. B **42**, 8928 (1990).